JMEPEG (2011) 20:399–404
DOI: 10.1007/s11665-010-9708-z

1059-9495/$19.00

Analyzing As-Cast Age Hardening of 356 Cast Alloy

Guiqing Wang, Liu Yan, Guocheng Ren, and Zhongkui Zhao

(Submitted January 29, 2010; in revised form June 6, 2010)

The as-cast age hardening behavior of 356 cast alloy has been investigated by micro hardness measurement, differential scanning calorimetry (DSC), transmission electron microscope (TEM), and electron probe micro analyzer. Age hardening results show that micro hardness value after as-cast aging treatment is almost the same as by T6 treatment, and the solidification rate has little effect on the as-cast age hardening response of 356 cast alloy. DSC and TEM analysis results show that the as-cast age hardening response of 356 cast alloy is attributed to the precipitation of β′ and β″ phases, the high Si concentration in α(Al) contributes about 10 HV to the micro hardness value for samples in as-cast and as-cast aging conditions.

Keywords age hardening, aluminum alloy, as-cast aging, precipitates

1. Introduction

Aluminum-silicon-magnesium alloys are of commercial importance because of a combination of excellent castability, achievable mechanical properties, good machinability, and light weight. The products obtained from these alloys are impellers, wheel hubs, pipes, casings, and a number of other parts. Chemical and heat treatments are applied to these alloys to obtain improved mechanical properties. The most common chemical treatment consists of modifying the morphology of the silicon eutectic phase from an acicular to a fibrous one by adding small amounts of sodium or strontium to the melts (Ref 1). This process improves mechanical properties, particularly the elongation percentage (Ref 2). As regards heat treatment, this process is used to obtain the desired combination of mechanical properties such as strength and ductility. The T6 treatment is the one which provides the best strength of these alloys. The standard T6 treatment comprises solution heat treatment, water quenching, and artificial aging. The main purpose of solution treatment and water quenching is to obtain a supersaturated solid solution which is responsible for the age hardening precipitation (Ref 3-6). The solution heat treatment is carried out at a relatively high temperature to fully dissolve the solutes into α(Al). This solution heat treatment may also have a significant impact on the microstructure, such as the coarsening of α(Al) and eutectic Si, which has a detrimental effect on the mechanical properties (Ref 7-9). In addition, the solution heat treatment is the most energy intensive stage.

In this article, the as-cast aging behavior of 356 (Al7Si0.3Mg) cast alloy is examined, which is aging the cast samples directly without solution treatment. The Mg and Si concentrations in α(Al) for samples with higher and lower solidification rate are analyzed, and the as-cast age hardening response and precipitation behaviors are investigated comparing with T6 treatment.

Guiqing Wang, Liu Yan, Guocheng Ren, and **Zhongkui Zhao**, Department of Material Science and Technology, Shandong Architectural University, Jinan 250101, People's Republic of China. Contact e-mail: wangguiqing@126.com.

2. Experimental Procedures

Commercial A356 ingots were used in preparation of experiment alloys. The experiment alloy was prepared in an electric resistance furnace. The melts were modified by Al-5Sr master alloy at 730 °C holding for about 30 min, and then held at 710 °C for about 10 min to ensure complete homogenization before pouring. Samples were cast in sand mold as shown in Fig. 1. Two Ni-Cr/Ni-Si thermocouples are placed in positions A and B of the mold to record the cooling speed. The measured cooling speed is about 10 °C/s in position A and 0.5 °C/s in position B. The examined specimens 1# to 9# were cut from side A to side B of the cast sample, which means cooling speed decreases progressively from 10 to 0.5 °C/s for 1# to 9# specimens. The chemical composition analyses for the experiment sample of A356 alloy are Si7.2wt.%, Mg0.31wt.%, Fe0.09wt.%, Sr0.041wt.%.

Hardness testing was carried out using a micro Vickers hardness tester with a load of 0.98 N and a dwell time of 15 s. Micro hardness test samples were lightly polished. Each micro hardness value was the average of at least five measurement results. The maximum hardness deviation of measurement is about 3 HV. Heat treatment was carried out in an electric furnace with a temperature control of ±3 °C. Differential scanning calorimetry (DSC) measurements were performed using a NETZSCH DSC 404 instrument. During DSC measurements, samples were protected under an argon atmosphere with a flow rate of 80 mL min^{-1}. S-type thermocouple has been used in DSC measurements. The measurements were performed from 25 to 650 °C at a heating rate of 10 °C min^{-1}. Superpure aluminum of similar mass to the sample was used as a reference, and the thermal events associated with phase transformations in the sample were analyzed after the subtraction of an appropriate baseline.

TEM specimens were thinned by mechanical polishing, followed by GL-69D ion-milling system. Argon ion with 4 kV,

0.4 mA was used in thinning the specimens until perforation. The Beam incidence angle on sample was 10-15°. TEM examination was carried out in an H-800 TEM transmission electron microscope operating at 150 kV. The precipitates identified by selected area elected area electron diffraction and energy dispersive spectrum (EDS). Quantitative analyses of solute concentration were conducted using JXA-8840 electron probe micro analyzer (EPMA).

3. Results and Analyses

3.1 As-Cast Age Hardening Analysis

The as-cast age hardening response has been examined by micro hardness measurements, i.e., heating the as-cast samples at 150 °C for 20 h. Micro hardness measurements on T4 and T6 treatment samples have been performed to compare the as-cast age hardening response. T4 treatment is solution heat-treating the as-cast samples at 530 °C for 8 h followed by water quenching and natural aging 24 h. The T6 treatment is heating the T4 samples at 150 °C for 20 h. Micro hardness measurement results on all specimens of 356 cast alloy are shown in Table 1 and Fig. 2. The micro hardness value increase ΔHV by artificial aging the as-cast samples and T4 samples at 150 °C for 20 h is also shown in Fig. 2, respectively. Micro hardness of Al7Si binary alloy has been examined as a reference.

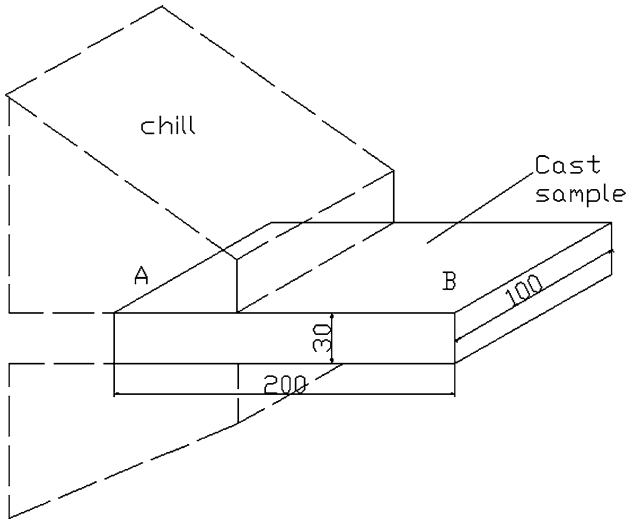

Fig. 1 Sand cast sample diagram (dimension unit: mm)

Table 1 Micro hardness value of samples with various solidification rates

Alloy type	Specimen code	Micro hardness (HV)			
		As-cast	As-cast aging	T4	T6
356 (Al7Si0.3Mg)	1#	79	86	55	87
	2#	71	81	59	94
	3#	78	89	63	95
	4#	77	86	63	84
	5#	70	91	65	89
	6#	77	86	62	88
	7#	77	85	70	88
	8#	76	91	67	89
	9#	80	95	70	94
Al7Si	10#	70	72	61	61

Comparing micro hardness data of various samples in as-cast and as-cast aging conditions are shown in Table 1 and Fig. 2, the cooling rate has little effects on micro hardness value in as-cast and as-cast aging conditions. Aging as-cast samples at 150 °C for 20 h directly, micro hardness value increases about 15%. The age hardening of Al-Si-Mg alloys is affected by the volume fraction, size and distribution of β″ and/or β′ phases precipitated during aging (Ref 10). The volume fraction of precipitates depends on the concentration of Mg and Si supersaturated in α(Al) before artificial aging that should be examined in Sect. 3.2.

The main purpose of T4 treatment is to obtain a maximum supersaturated solution. Alloys are generally strengthened by T4 treatment, and maximum age hardening response has been obtained by T6 treatment. However, the micro hardness experiment results show that micro hardness value decreases after T4 treatment for all samples (see Table 1; Fig. 2). Micro hardness increase value ΔHV by aging T4 samples at 150 °C for 20 h is higher than that by aging the as-cast sample, but the micro hardness values for samples by as-cast aging treatment are almost the same as samples by T6 treatment. These may be related to Mg and Si concentrations and precipitation in α(Al) and has been analyzed in following sections.

3.2 Concentrations of Mg and Si Supersaturated in a(Al)

For as-cast samples, the solid solubility of Mg and Si in α(Al) should be related to the solidification conditions. Figure 3(a) and (b) shows microstructures and Mg and Si concentrations in α(Al) for both as-cast samples by electron probe micro-analysis. Data in Fig. 3(a) is from the sample solidified in highest rate and data in Fig. 3(b) is from the sample solidified in lowest rate. The values of Si concentration near edge of the dendrite are not shown due to influence of surrounding Al-Si eutectic.

It can be seen from Fig. 3 that Mg concentration supersaturated in α(Al) for as-cast samples of 356 alloy is about 0.25 wt.% and the cooling rate has little effects on the Mg

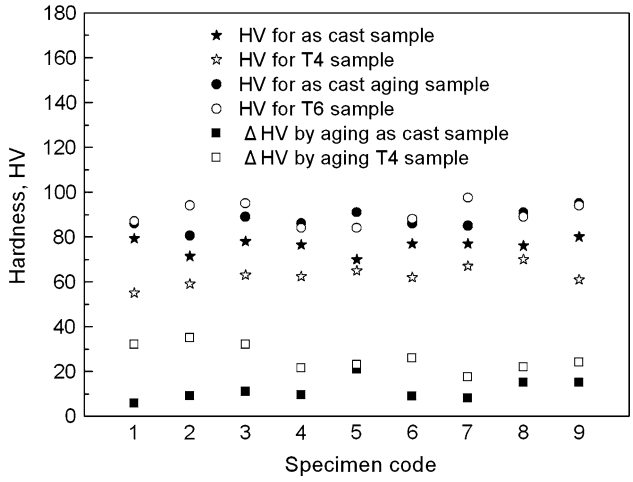

Fig. 2 Micro hardness value for samples 1# to 9# in various conditions and micro hardness increase value ΔHV

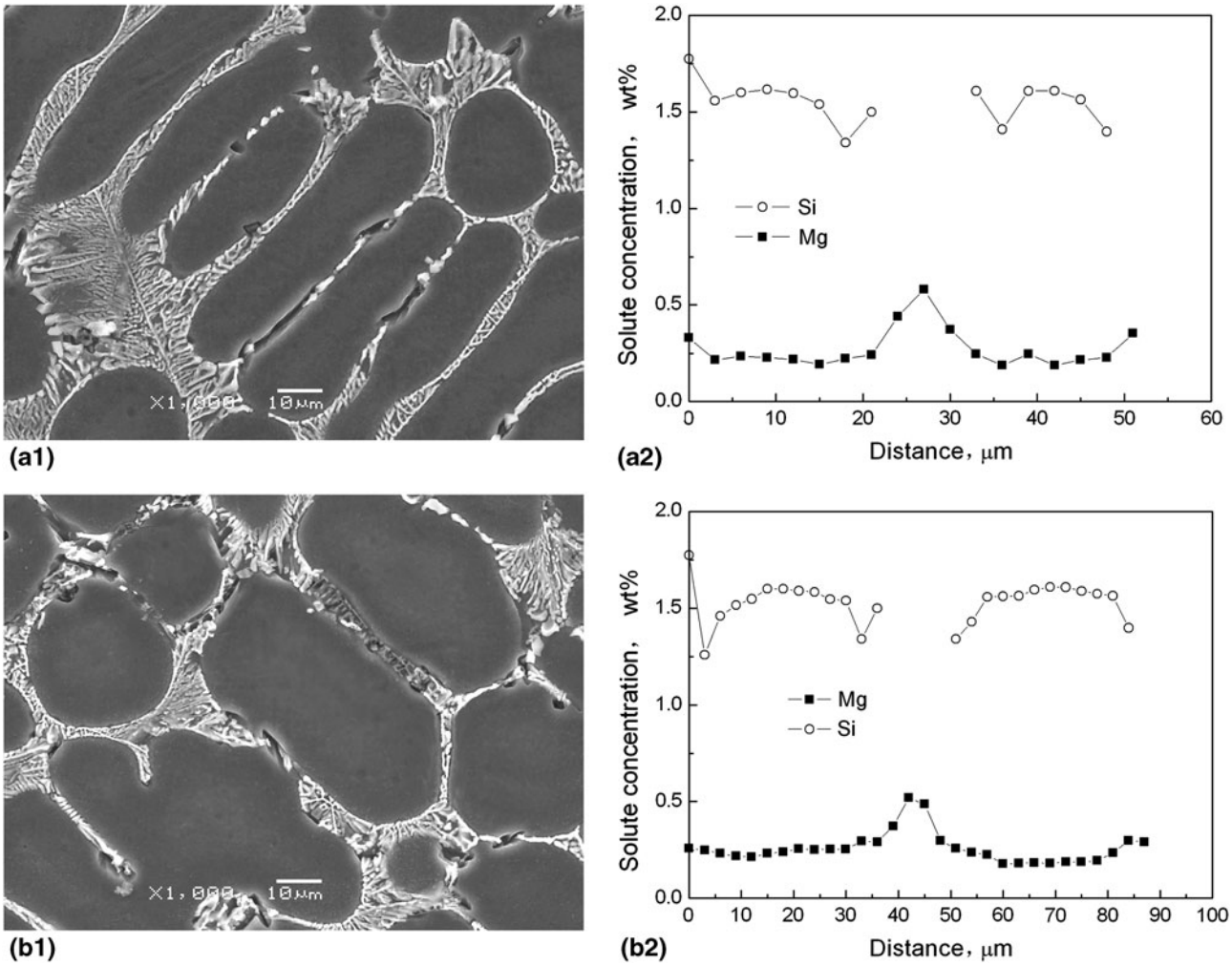

Fig. 3 Microstructure and distribution of Si and Mg across the dendrites for 356 cast samples with higher (a) and lower (b) solidification rates

concentration supersaturated in α(Al). It is strange that the Si concentration supersaturated in α(Al) for as-cast samples of 356 cast alloy is about the maximum solid solubility 1.6 wt.% of Si in α(Al) and anti-segregation occurs. This phenomenon should be related to solidification characteristics of Al-Si cast alloys. Dons et al. explain that the "anomalous" microsegregation within dendrites in Al-Si cast alloys caused by the growth of eutectic Si particles after solidification result in a reduction of Si in solid solution in dendrites in the vicinity of the eutectic (Ref 11, 12).

For Al-Si-Mg samples with Mg and Si supersaturated in α(Al), diffusion and precipitation should occur during aging. Aging both of the examined as-cast samples at 150 °C for 20 h, the Mg and Si concentration in α(Al) are shown in Fig. 4.

Comparing Fig. 4 with 3, distribution and concentration of Mg in α(Al) dendrites change little, which means that Mg-related precipitation during as-cast age hardening stage occurs within α(Al). Moreover, distribution and concentration of Si in α(Al) dendrites change clearly, and there is a trend of Si supersaturated in α(Al) diffusing to dendrite edges during this as-cast aging stage. Moreover, there is yet high Si supersaturated in α(Al) after aging at 150 °C for 20 h.

Figure 5 shows the Mg and Si concentration in α(Al) for T4 (solution treating at 530 °C for 8 h followed by water quenching) and T6 samples (artificial aging T4 samples at 150 °C for 20 h). Comparing Fig. 5(a) with Fig. 3 and 4, the Mg concentration supersaturated in α(Al) is almost the same as the Mg content in alloy compositions after T4 treatment, Si homogenously distributes in α(Al) with the concentration 1.0 wt.%, which is the maximum solid saturation of Si in α(Al) at 530 °C. Comparing Fig. 5(a) with (b), the Mg and Si concentrations in α(Al) change little after artificial aging T4 samples at 150 °C for 20 h, which means that aging precipitation only occurs within α(Al) during this artificial aging.

Micro hardness measurement results in Table 1 shows that micro hardness value for Al7Si binary alloy sample in T4 and T6 conditions is about 10 HV lower than that in as-cast and as-cast aging conditions, and micro hardness value changes little after as-cast aging or aging T4 sample. The little micro hardness value changes of Al-Si binary alloy by aging as-cast samples and T4 samples suggest that the Si precipitation during aging has little effect on age hardening response because only Si precipitation occurs during aging this Al-Si binary.

For the Al-Si binary alloy, T4 treatment should only accompany with the changes of Si concentration in α(Al) like that of 356 (Al7Si0.3Mg) alloy, as shown in Fig. 5(a) with Fig. 3(a). The decrease of micro hardness value after T4 treatment of Al7Si binary alloy suggests that the anomalous

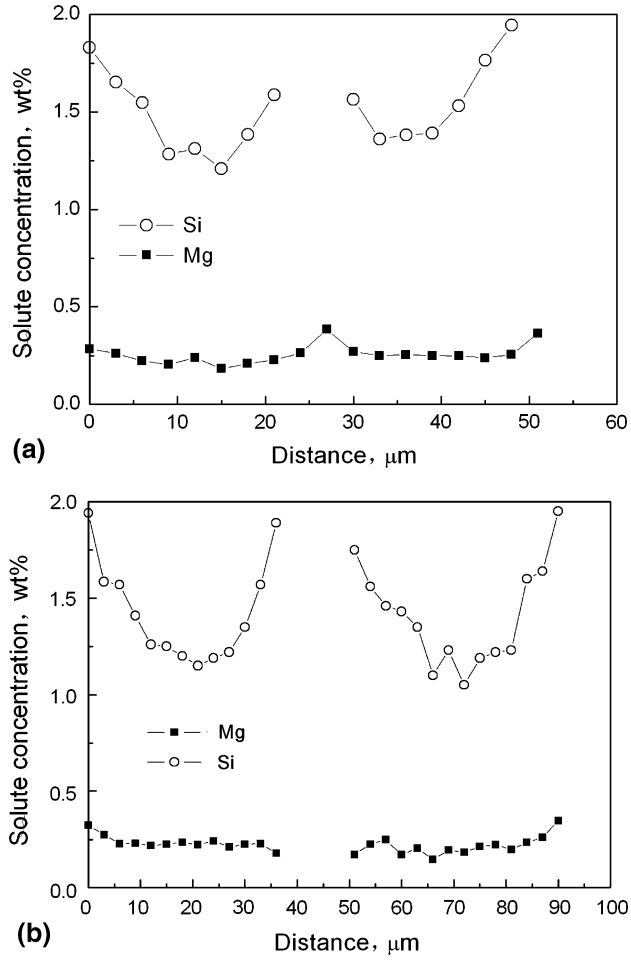

Fig. 4 Distribution of Si and Mg across the dendrites of 356 specimens as-cast aging at 150 °C for 20 h. Sample cast with higher (a) and lower (b) solidification rates

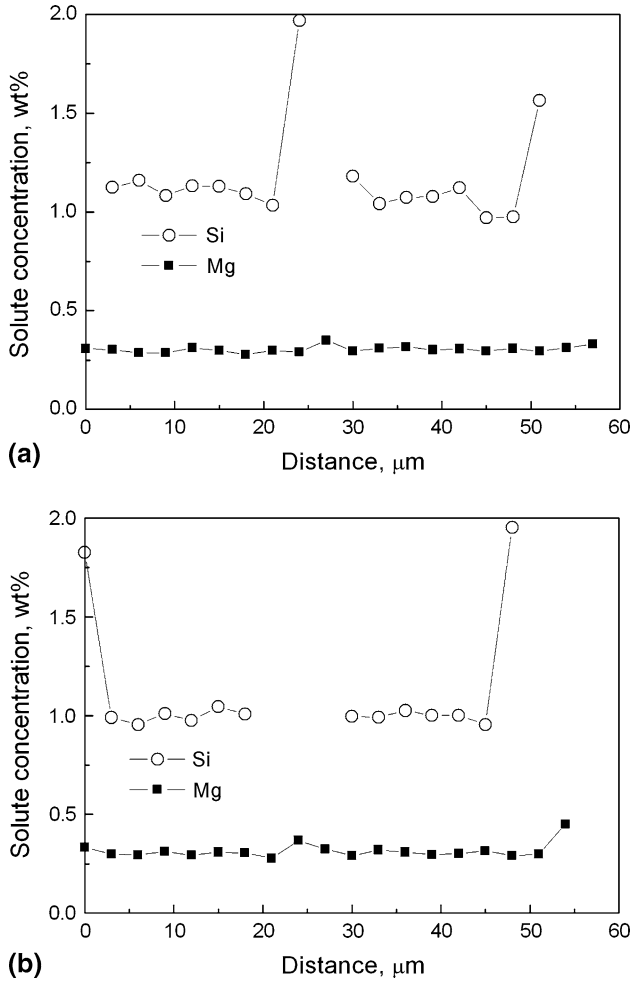

Fig. 5 Distribution of Si and Mg across the dendrites for 356 alloy (a) T4 sample and (b) T6 sample

high Si concentration within α(Al) for as-cast and as-cast aging samples makes contribution to micro hardness of α(Al) and this contribution decreases when Si concentration changes to normal supersaturation after solution treatment.

3.3 Age Precipitation Behaviors

In a DSC experiment, the rate of heat evolution (or absorption) is plotted as a function of temperature. The precipitation event is manifested as an exothermic peak, and the melting event is manifested as an endothermic peak. For a given heating rate, the peak temperature depends upon the specific precipitation or melting process.

DSC trace obtained by heating the as-cast specimen is shown in Fig. 6. DSC measurement for heating T4 specimen is carried out as a reference. The age hardening state of Al-Si-Mg alloys is generally considered to be associated with the precipitation of GP zones, β″ and/or β′ transitional phases in α(Al) (Ref 13-16). DSC traces as shown in Fig. 6 exhibited two exothermic peaks over-lapped in the temperature range of 180-320 °C. Previous DSC investigations on Al-Mg-Si alloys (Ref 17-20) showed that exothermic peak in the temperature range of 180-260 °C corresponded to the precipitation of coherent β″ phase, exothermic peak in the temperature range of 260-320 °C was caused by the precipitation of semi-coherent β′ phase. The DSC trace of T4 specimen shows higher β″ precipitation peak (see Fig. 6), which means that there should be more β″ precipitates hardening the alloy during aging the T4 sample. This is consistent with the micro hardness measurement results shown in Fig. 2 that micro hardness increase value ΔHV by aging T4 samples is higher than that by aging the as-cast sample. Exothermic peaks at around 100-150 °C corresponded to the precipitation of GP zone are not detected in both DSC traces, which means that precipitation of GP zones might occurred before heating. A endothermic peak with the onset temperature 150 °C appears in DSC trace of T4 specimen, which should be related to the dissolution of GP zones. This means that some GP zones precipitated in T4 samples might not be big enough as the nucleus of β″ phase and these GP zone should dissolve when aging temperature higher than 150 °C. For DSC trace of as-cast specimen, endothermic peak of GP zones are not detected, which means that there are not GP zones dissolving during as-cast aging and GP zones precipitated in as-cast samples should be as nucleus of β″ phase.

Figure 7 shows a TEM micrograph and the corresponding selected area electron diffraction pattern for an as-cast specimen of 356 alloy. The image contrast should be the crystal distortion due to the precipitation of GP zones coherent with α(Al). This means that GP zones have exist in the as-cast samples, which

might precipitate during the cooling stage of castings or the natural aging stage before artificial aging. Aging as-cast samples with this structure, GP zones should be as nucleus of β″ and/or β′ phases.

Figure 8 shows a TEM micrograph and the corresponding selected area electron diffraction pattern for an 356 cast specimen directly aging at 150 °C for 20 h. Needle-like precipitates are β′ phase semi-coherent with α(Al), image contrast are caused by β″ phase coherent with α(Al) by analyzing the corresponding selected area electron diffraction pattern. In addition, spherical Si phases with diameters of tens nanometers appear. It can be seen that many precipitates are curved. There are many dislocations formed in α(Al) of Al-Si cast alloys because of the different contraction coefficient of Al and Si. These curved precipitates should form along dislocations. The TEM results suggest that the as-cast age hardening of 356 alloy is attributed to the precipitation of β′, β″, and spherical Si phases. The β′ and β″ phases are known to be the hardening precipitates of these type alloys (Ref 13-16), and the Si precipitation is generally considered to be little contribution on age hardening, but has solution strengthening on α(Al) as analyzed in upper sections. It is difficult to compare the number and size of precipitates for samples after as-cast aging with that after T6 treatment by TEM micrographs, because of the wide size range and curved shape of precipitates.

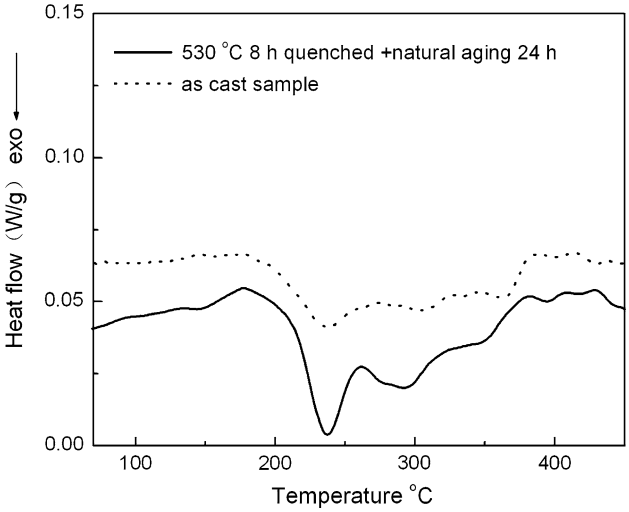

Fig. 6 DSC curves for samples at a heating rate of 10 °C min^{-1}

4. Discussions

It is generally realized that high solidification rate is beneficial on strength properties of castings because of the fine microstructure. The experiment results in this article

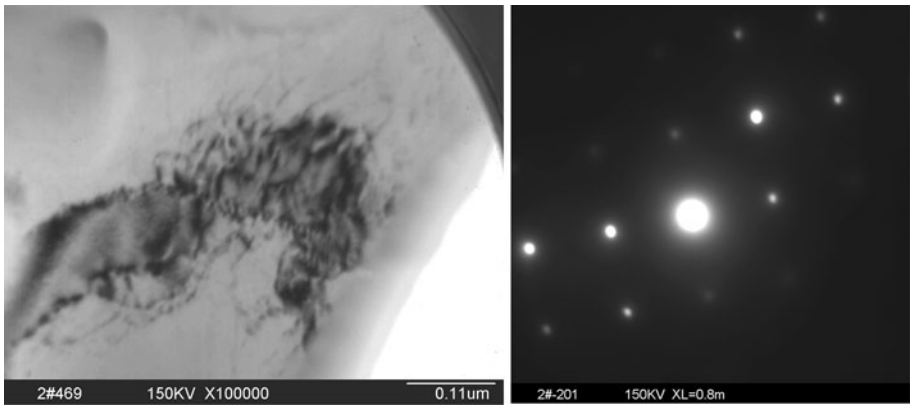

Fig. 7 TEM micrograph for as-cast sample of 356 alloy

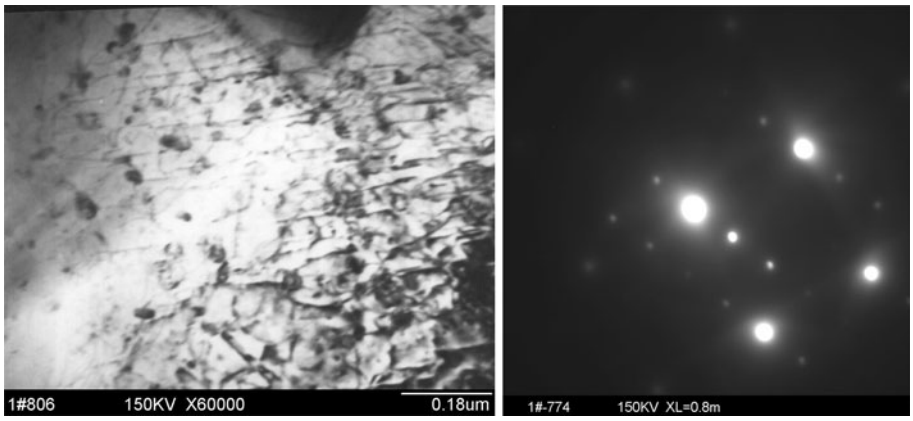

Fig. 8 TEM micrographs for sample of 356 alloy as-cast aging at 150 °C 20 h

show that there is poor correlation between micro hardness and solidification rate as shown in Table 1, which may be related to the factors influencing micro hardness of Al-Si-Mg cast samples. For Al-Si-Mg cast samples, strength properties are influenced by many factors, such as Si morphology, dendrite arm spacing, shrinkage defects, pore, and inclusions, but the micro hardness of α(Al) is mainly related to the characteristics of α(Al), such as α(Al) grain size, solubility of alloy elements in α(Al), nanometer precipitates (Ref 1, 21). For as-cast samples, micro hardness is mainly influenced by the solubility of Si and Mg in α(Al). For aging samples, micro hardness is influenced by the solubility of Si and Mg in α(Al) and the nanometer phases precipitated in α(Al). Because of this characteristic, micro hardness is generally used as measuring the age hardening response of aluminum alloys. Data in Fig. 3 shows that there should be about 0.25 wt.% Mg supersaturated in α(Al) in ordinary casting conditions, and the solidification rate has little effects on Mg and Si concentration supersaturated in α(Al). This is consistent with the poor correlation between micro hardness and solidification rate. For Al-Si-Mg cast alloys, the age hardening response depends on the Mg contents. More than 0.25 wt.% Mg is often added to Al-Si-Mg alloys to obtain high age hardening response. For Al-Si-Mg alloy with more than 0.25 wt.% Mg, Mg_2Si phases should formed in grain boundaries (Ref 22, 23). It is known that the Mg_2Si phase in grain boundaries has little hardening ability and is harmful on alloys tensile properties. For 356 cast alloy, there are a little of Mg_2Si phases in grain boundaries. For higher Mg-containing Al-Si-Mg cast alloys, T6 treatment is necessary to decrease the harmful effect of Mg_2Si phase in grain boundaries on alloys tensile properties. The age hardening of more than 0.25 wt.% Mg on α(Al) are achieved by T6 treatment.

5. Conclusions

(1) For 356 samples, micro hardness value by as-cast aging treatment is almost the same as by T6 treatment, and the solidification rate has little effect on the as-cast age hardening response.
(2) The solidification rate has little effects on the Mg concentration supersaturated in α(Al). The Si concentration supersaturated in α(Al) in as-cast samples of 356 cast alloy is about 1.6 wt.%. Aging as-cast samples at 150 °C for 20 h, the distribution and concentration of Mg in α(Al) changes little, and there is yet higher Si supersaturated in α(Al).
(3) The as-cast age hardening response of 356 alloy is attributed to the precipitation of β′ and β″ phases, the high Si concentration in a(Al) contributes about 10 HV to the micro hardness value of as-cast and as-cast aging samples.

Acknowledgments

We gratefully acknowledge the support of Shandong Science and Research Foundation for Middle and Young People (Grant No. 2008BS05002) and Shandong Provincial Natural Science Foundation of China (Grant No. Y2007F39).

References

1. K.T. Kashyap, S. Murali, K.S. Raman, and K.S.S. Murthy, Overview, Casting and Heat Treatment Variables of Al-7Si-Mg Alloy, *Mater. Sci. Technol.*, 1993, **101**, p 189–203
2. S. Shivkumar, L. Wang, and C. Keller, Notched Tensile Properties of Heat-Treatment A356 Castings, *AFS Trans.*, 1995, **103**, p 705–709
3. D.L. Zhang, L.H. Zheng, and D.H. StJohn, Effect of a Short Solution Treatment Time on Microstructure and Mechanical Properties of Modified Al-7wt.%Si-0.3wt.%Mg Alloy, *J. Light Met.*, 2002, **2**, p 27–36
4. D. Apelian, S. Shivkumar, and G. Sigworth, Fundamental Aspects of Heat Treatment of Cast Al-Si-Mg Alloys, *AFS Trans.*, 1989, **97**, p 727–742
5. O.S. Es-Said, D. Lee, W.D. Pfost, D.L. Thompson, M. Patterson, J. Foyos, and R. Marloth, Alternative Heat Treatments for A357–T6 Aluminum Alloy, *Eng. Fail. Anal.*, 2002, **9**, p 99–107
6. E.N. Pan, J.F. Hu, and C.C. Fan, Solution-Treatment Conditions for Optimal Tensile Properties in A357 Alloy, *AFS Trans.*, 1996, **104**, p 1119–1131
7. P.Y. Zhu, O.Y. Liu, and T.X. Hou, Spheroidization of Eutectic Silicon in Al-Si Alloys, *AFS Trans.*, 1983, **91**, p 609–614
8. D.L. Zhang, L.H. Zheng, and D.H. Stjohn, Effect of Solution Treatment Temperature on Tensile Properties of Al-7Si-0.3 Mg(wt%) Alloy, *Mater. Sci. Technol.*, 1998, **14**, p 619–625
9. E. Ogris, A. Wahlen, H. Lüchinger, and P.J. Uggowitzer, On the Silicon Spheroidization in Al–Si Alloys, *J. Light Met.*, 2002, **2**, p 263–269
10. Q.G. Wang and C.J. Davidson, Solidification and Precipitation Behaviour of Al-Si-Mg Casting Alloys, *J. Mater. Sci.*, 2001, **36**, p 739–750
11. A.L. Dons, L. Pedersen, and L. Arnberg, The Origin of "Anomalous" Microsegregation in Al-Si Foundry Alloys-Modelling and Experimental Verification, *Mater. Sci. Eng.*, 1999, **A271**(1–2), p 91–94
12. L. Pedersen and L. Arnbery, Anomalous Microsegregation in Al-Si Foundry Alloys, *Mater. Sci. Eng.*, 1998, **A241**(1–2), p 285–289
13. G.A. Edwards, K. Stiller, and G.L. Dunlop, The Precipitation Sequence in Al-Mg-Si Alloys, *Acta Mater.*, 1998, **46**(11), p 3893–3904
14. C.S. Tsao, C.Y. Chen, and U.S. Jeng, Precipitation Kinetics and Transformation of Metastable Phases in Al-Mg-Si Alloys, *Acta Mater.*, 2006, **54**(17), p 4621–4631
15. M. Murayama and K. Hono, Pre-Precipitate Clusters and Precipitation Processes in Al–Mg–Si Alloys, *Acta Mater.*, 1999, **47**, p 1537–1548
16. S.P. Yuan, G. Liu, and R.H. Wang, Aging-dependent Coupling Effect of Multiple Precipitates on the Ductile Fracture of Heat-treatable Aluminum Alloys, *Mater. Sci. Eng. A*, 2009, **A499**(1–2), p 387–395
17. A. Gaber, M.A. Gaffar, M.S. Mostafa, and E.F. Abo Zeid, Precipitation Kinetics of Al-1.12Mg2Si-0.35Si and Al-1.07Mg2Si-0.33Cu Alloys, *J. Alloys Compd.*, 2007, **429**, p 167–175
18. W.F. Miao and D.E. Laughlin, A Differential Scanning Calorimetry Study of Aluminum Alloy 6111 with Different Pre-aging Treatments, *Journal of Materials Science Letters*, 2000, **19**(3), p 201–203
19. L. Zhen and S.B. Kang, DSC analyses of the Precipitation Behavior of Two Al-Mg-Si Alloys Naturally Aged for Different times, *Mater. Lett.*, 1998, **37**, p 349–353
20. X.R. Zuo and Y.W. Jing, Investigation of the Age Hardening Behaviour of 6063 Aluminium Alloys Refined with TI, RE and B, *J. Mater. Process. Technol.*, 2009, **209**(1–2), p 360–366
21. L.F. Mondolfo, Aluminum Alloys: Structure and Property (in Chinese), W. Zhutang, Z. Zhenlu, X. Zheng, Pub. Metallurgical industry Press, Beijing, 1988, p 239–240, 203–204, 586–593
22. D.L. Zhang and L.H. Zheng, The Quench Sensitivity of Cast Al-7Wt Pct Si-0.4 Wt Pct Mg Alloy, *Metall. Mater. Trans. A*, 1996, **27A**(12), p 3843–3991
23. R.I. Mackay and J.E. Gruzleski, Quantification of Magnesium in 356 Alloy via Thermal Analysis, *Int. J. Cast Metals Res.*, 1998, **10**, p p255–p265